Eur. Phys. J. B **59**, 399–403 (2007)
DOI: 10.1140/epjb/e2007-00293-1

THE EUROPEAN PHYSICAL JOURNAL B

Randomness and a step-like distribution of pile heights in avalanche models

A.B. Shapoval[1,2,a] and M.G. Shnirman[1,3]

[1] International Institute of Earthquake Prediction Theory and Mathematical Geophysics, Warshavskoye sh. 79, kor. 2, Moscow, 117556, Russia
[2] Finance Academy under the Government of the Russian Federation, Leningradsky pr. 49, 125468, Moscow, Russia
[3] Institut de Physique du Globe de Paris, 4, place Jussieu, 75252 Paris, France

Received 31 May 2006 / Received in final form 14 September 2007
Published online 1st November 2007 –

Abstract. This paper considers a one-parameter family of sand-piles. The family exhibits the crossover between the models with deterministic and stochastic relaxation. The mean pile height is used to describe the crossover. The height densities corresponding to the models with relaxation of both types approach one another as the parameter increases. Relaxation is supposed to deal with the local losses of grains by a *fixed amount*. In that case the densities show a step-like behaviour in contrast to the peaked shape found in the models with the local loss of grains down to a *fixed level* [S. Lübeck, Phys. Rev. E **62**, 6149 (2000)]. A spectral approach based on the long-run properties of the pile height considers the models with deterministic and random relaxation more accurately and distinguishes between the two cases for admissible parameter values.

PACS. 05.70.Jk Critical point phenomena – 05.65.+b Self-organized systems

1 Introduction

In 1987 Bak et al. (BTW) introduced their sand-pile model [1]. The model involves a system containing some physical quantity called sand in the original paper. The system is slowly loaded. Extra loading results in a local relaxation. The local relaxation releases energy that can instantly spread out to large distances. The spreading mechanism is fully deterministic. The model's system achieves its critical state without adjusting any parameter [2].

Numerous power laws describe the critical state. They have been established theoretically [3,4] and numerically [5–7]. The model laws find their application in such different fields as neural networks [8], earthquakes [9], and solar flares [10].

A great demand for the model has resulted in its modifications. The versions that are the closest to the original sand-pile model are probably Manna's and Zhang's models [11,12]. Manna has defined the spreading of a local relaxation in a stochastic way. Zhang has introduced a continuous sand-pile. The critical behaviour of these models exhibits certain similarities. Since minor changes in the rules of the model little affect the critical behaviour [13] and the number of changes is inexhaustible, the models need a strict classification.

[a] e-mail: shapoval@mccme.ru

Many papers assign the models to the same universality class, if they have the same set of exponents determining the critical power laws [13]. The lively debate [14–18] using different approaches has arrived at the conclusion that BTW's and Manna's sand-piles belong to different universality classes [19]. Preliminary investigation suggests that the BTW and Zhang sand-piles should represent the same universality class [20].

The paper [21] introduced a family of models realizing the crossover between Manna's and Zhang's sand-piles. The control parameter is closely related to local energy relaxation. Small values of the energy characterize the Manna model, while extremely large values lead to Zhang-type behaviour.

Local relaxation is defined for Lübeck's sand-piles [21] in terms of energy loss down to a *fixed level*. The family of sand-piles in [22] deals with the loss of energy by a *fixed amount*.

The family of models in [22] enables the crossover between the BTW sand-pile and the random walk with some modification of the Manna sand-pile in-between. This crossover corresponds to the relatively small energy mentioned above. On the other hand, the family determines a sophisticated limit behaviour as the energy tends to infinity. The classification based on the power laws fails to describe the great diversity that this continuous sand-pile

family involves. De los Rios and Zhang [23] introduce an appropriate global functional whose evolution calculated in terms of the spectrum determines the system dynamics.

Karmakar et al. [24] introduce an energy propagation mechanism that lacks local symmetry, thus leading to sand-piles with controlled disorder. These models depend on some parameter that defines the asymmetry. The BTW sand-pile belongs to these models and corresponds to an absense of asymmetry. Establishing the deterministic relaxation, the Karmakar et al. [24] family of models essentially differs from those of [21] and [22]. The properties of this family have been found, but the crossover to the BTW sand-pile is not considered.

In this paper we investigate the sand-pile family of [22]. The relevant sand distribution is found to be essentially different from the distribution appearing in the models usually discussed, in particular, in Zhang's and Lübeck's models. As the control parameter is relatively large, the difference between deterministic and stochastic relaxation almost disappears, and the sand distribution over the system proves to be similar for both types of models. However, the spectral properties select the sand-piles with the deterministic relaxation.

2 The model

The model involves a two-dimensional square lattice $L \times L$. Each cell contains h_{ij} grains, where h_{ij} is less than an integer threshold H. At every time moment, a cell (i, j) is chosen at random. Its number of grains (referred to as height) h_{ij} increases by 1:

$$h_{ij} \longrightarrow h_{ij} + 1.$$

If the resulting height h_{ij} remains less than H, then nothing more happens at the moment. Otherwise, the cell (i, j) becomes unstable and relaxes. Relaxation depends on an integer control parameter n. An unstable cell distributes its n grains "in equal parts" among its 4 nearest neighbours. Namely, when $n = 4k$, each neighbour gets exactly k grains.

Naturally, there exist numbers $n = 4k + r$, where the residue $r < 4$ is not equal to zero. Then each neighbour gets k grains and the remaining r grains are given to the four different neighbours at random. The following formula expresses the idea of this construction:

$$\begin{aligned} h_{ij} &\longrightarrow h_{ij} - n, \\ h_{\text{neighbour}(i,j)} &\longrightarrow h_{\text{neighbour}(i,j)} + k \quad \text{or} \\ h_{\text{neighbour}(i,j)} &\longrightarrow h_{\text{neighbour}(i,j)} + k + 1. \end{aligned}$$

During relaxation other cells can achieve the threshold H and become unstable, relaxing according to the same rules. If a boundary cell relaxes, $[n/4]$ or $[n/4] + 1$ grains leave the lattice and dissipate, where $[x]$ is the integer part of x. (The dissipation is higher for the corner cells).

Successive acts of relaxation constitute an *avalanche*. The *size* of any avalanche is the number of unstable cells during the avalanche counted according to their multiplicity. The dissipation at the boundary assures that the avalanches are defined correctly and their size is finite.

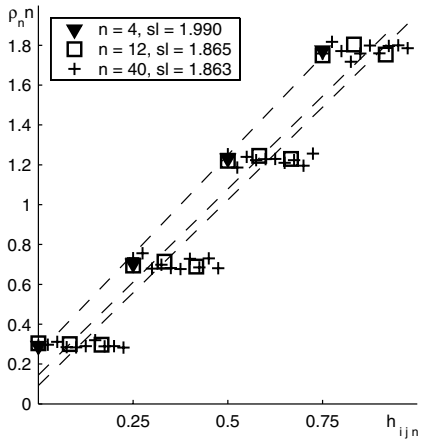

Fig. 1. Normalized height density; the dashed lines are linear fits; their slopes (sl) are given in the legend; $L = 256$.

The case $n = H = 4$ corresponds to the original sand-pile of [1]. It is worth noting that [21] introduces a relaxation involving the loss of any unstable cell down to a fixed level. To be specific, $h_{ij} \longrightarrow H - n$ and h_{ij} grains are passing one-by-one to the nearest neighbours; the receiver for each grain is found at random. These changes in the rules qualitatively influence the system. The limiting behaviour ($n \to \infty$) for the [21] family and the models discussed above is different.

Our family really depends on the parameter n only. The values of H do not affect the system dynamics. They determine the admissible interval $[H - n, H)$ of heights. Our simulation deals with $H = 4$, while the total number of the grains added is $2^{20}n$.

3 Pile height densities

Following the ideas of [21], we establish some features of the sand distribution over the lattice. Let the normalized heights h_{ijn} be $h_{ijn} = (h_{ij} - H + n)/n$. Then $h_{ijn} \in [0, 1)$. Further, $\rho_n(k/n)$ is defined as the number of h_{ijn} equal to k/n. Then the normalized function $n\rho_n(k/n)$ can be treated as a probability density (we use this term, even though the distribution is discrete). According to Figure 1, the densities $\rho_n(\cdot)n$ follow four flat steps with a high accuracy for $n = 4k$. The steps correspond to the values of the density $4\rho_4$ for the BTW sand-pile. (The points of ρ_4 shown in Figure 1 are in good agreement with the exact values found in [25].)

Each density is fitted by a linear function (Fig. 1). Their slopes (sl in the legend) slightly decrease with n increasing and must be saturating as n tends to infinity.

The following construction manages to compare quantitatively the four steps of $\rho_n(\cdot)$ for $n > 4$ with the four values of $\rho_4(\cdot)$ representing the BTW sand-pile. Given $n = 4, 5, \ldots$, the values of the function $\rho_n(\cdot)$ are sampled into four bins $[0, 0.25)$, $[0.25, 0.5)$, $[0.5, 0.75)$, and

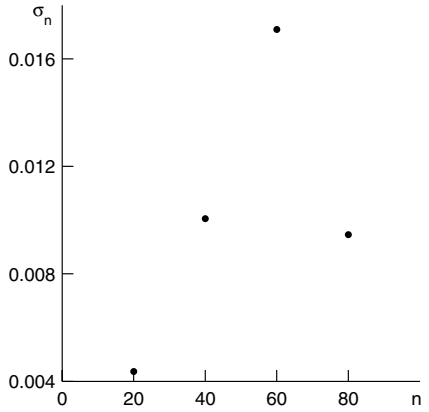

Fig. 2. Difference between the steps of ρ_n and the function ρ_4 measured by the functional σ_n.

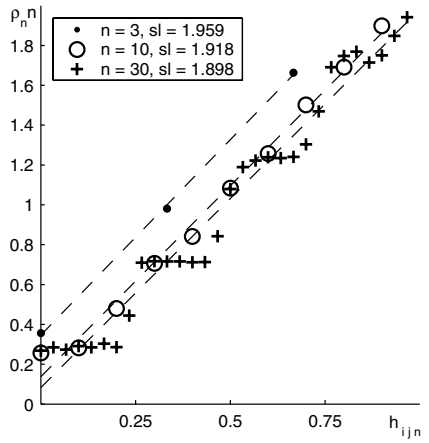

Fig. 3. Height density; the dashed lines are linear fits, $L = 256$; their slopes (sl) are in the legend.

$[0.75, 1)$ with the respective values of $\psi_n(\cdot)$ being ascribed to 0, 0.25, 0.5, and 0.75. For example, $\psi_n(0) = \rho_n(0) + \rho_n(1/n) + \ldots + \rho_n(j_0/n)$, where j_0 is the biggest integer with $j_0/n < 0.25$. In particular, $\psi_4(\cdot)$ coincides with $\rho_4(\cdot)$. Then $\psi_n(\cdot)$ is defined at 4 points. Each value of $\psi_n(k/4)$, $k = 0, 1, 2, 3$, represents one step of $\rho_n(\cdot)$.

Let

$$\sigma_n = \sqrt{\sum_{k=0}^{3} \left(\psi_n(k/4) - \rho_4(k/4)\right)^2 / 3}$$

Then σ_n measures the difference between the steps and the function $\rho_4(\cdot)$ corresponding to the BTW sand-pile.

The difference from the BTW sand-pile increases with increasing σ_n (Fig. 2). These values of σ_n indicate that there exists a certain maximum of the difference corresponding to $n \approx 60$. This observation agrees with the change in the tendency exhibited by the sand-pile family of [21] for the intermediate values of the control parameter.

In the same way, the densities are introduced to develop models with $n \neq 4k$ starting from $n = 3$. A computer experiment proves (Fig. 3) that the densities $n\rho_n$ quickly (with n increasing) are aligned in four steps of $4\rho_4$. The linear fits have slopes that are close to that for ρ_{4k}.

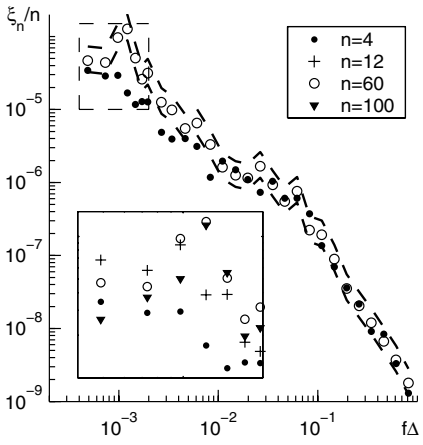

Fig. 4. Normalized spectrum ξ_n/n vs normalized frequency $f = f_k$. The inset contains the graphs in the boxed part of the figure; $\Delta = 8n$, $N = 16$, $r = 8192$, $L = 256$. The dashed lines indicate the error interval for the circles.

The following reasoning gives a rough explanation of the step-like behaviour of the densities. Given the parameter value n, the heights are naturally divided into four intervals $[H - n, H - 3n/4)$, $[H - 3n/4, H - n/2)$, $[H - n/2, H - n/4)$, $[H - n/4, H)$, since each act of relaxation maps one interval onto another (possibly excepting the boundary values due to the random effect). The normalization (on n) transforms these intervals to the domain of definition of the four steps shown in Figures 1 and 3.

It is worth noting that the sand-piles of [12,21] demonstrate peaked densities of the average height in contrast to our ρ_n.

In terms of the sand distribution, therefore, the family exhibits a certain similarity. The densities ρ_n for $n = 4k$ and $n \neq 4k$ become almost indistinguishable, when n has the order of a few tens.

4 A spectral approach

Another approach gives evidence of the diversity of the two cases ($n = 4k$ and $n \neq 4k$). It deals with the spectrum of the average height $h = L^{-2} \sum_{i,j=1}^{L} h_{ij}$. The average height is calculated at the end of every time moment and treated as a function of time, $h(t)$. The spectrum of $h(t)$ is successfully used in [23] to describe the authors' sand-pile dynamics. Our spectrum of $h(t)$ appears to be noisy, therefore it has been averaged over several realizations. Besides, each realization is stored in the bins of some length Δ. Then the Fourier transform determines the spectrum ξ. The highest frequency is $1/\Delta$ in the case considered.

The formal procedure used to calculate the spectrum consists of four steps.

1. For some fixed N the time moments for which $h(t)$ is catalogued are divided into N non-intersecting intervals of the same length T.

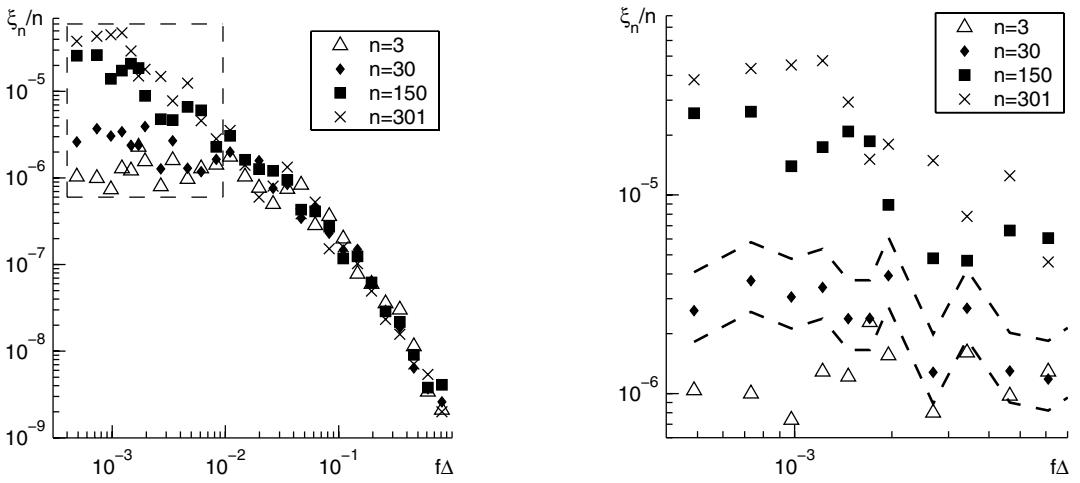

Fig. 5. Normalized spectrum ξ_n/n vs normalized frequency $f = f_k$; $\Delta = 8n$, $N_R = 16$, $r = 8192$, $L = 256$ (a) full graph, (b) box in panel a. The dashed lines indicate the error interval for the diamonds.

2. For any fixed interval (step 1), the values of $h(t)$ are averaged over relatively small subintervals. This reduces the number of data for subsequent numerical application of the fast Fourier transform. Let Δ be the length of the small subintervals and r be their number, $r\Delta = T$. Then a signal x_j is defined as the arithmetic mean of all the $h(t)$-values in the j-th subinterval, $j = 1, 2, \ldots, r$.
3. The spectrum of x_j is determined in terms of the Fourier transform:

$$\hat{x}_k = \frac{1}{\sqrt{r}} \sum_{j=1}^{r} \big(x_j - \langle x \rangle\big) e^{-\frac{2\pi i k j}{r}},$$

where $\langle x \rangle$ is the mean of x_j, $j = 1, \ldots, r$, $i = \sqrt{-1}$. Then the frequencies f_k are $k/(r\Delta)$, $k = 1, 2, \ldots, r$, and the power spectrum $\xi(f_k)$ of the signal x_j is defined as $\xi(f_k) = |\hat{x}_k|^2$.
4. Each of N intervals defined at step 1 generates its own spectrum $\xi(f_k)$. The averaging of $\xi(f_k)$ results in a stabilized spectrum, which we wanted to obtain. The stabilized spectrum depends on the model parameter n. Thus, the notation $\xi_n(f_k)$ is still valid for the stabilized spectrum.

According to [22], the family of spectra admits of a certain normalization. If Δ is proportional to n, the plot of $\xi_n(f_k)/n$ versus dimensionless frequency $f_k\Delta$ shows that the graphs at high frequencies coalesce (Fig. 4). The scaling of axes in Figure 4 remains reasonable for the other frequencies.

Leaving aside the main part of the spectrum, we will attend to some interval of low frequencies. The corresponding part of the graphs is boxed in Figure 4 and shown in the inset. In this part of this figure the curves of ξ_n/n for small n are higher for larger n. When $n \approx 60$, the tendency is changed. The curve of ξ_n/n is close to that of $\xi_4/4$ at the leftmost points in the figure. However, in contrast to $\xi_4/4$, has a maximum. The change in tendency for $n \approx 60$ agrees with the behavior shown by the family of functions of σ_n discussed above.

The horizontal coordinates of this box are not absolute constants. They depend on the lattice length L and the simulation time. As L increases, the box moves to the left, becoming invisible in Figure 4.

The influence of the simulation time is essential. The investigated part of the spectrum reflects the frequencies of rare, large, and strongly dissipative avalanches. The lack of data limits the results for these avalanches. This remark agrees with the partial conclusions about the rare avalanches for the BTW and Manna sand-piles [26].

In contrast to the quick convergence of $\rho_n n$, $n \neq 4k$ to their four values, the family ξ_n/n of spectra exhibits quite a different tendency. Since the high-frequency spectra are rather similar (Fig. 5a), the analysis focuses on the low frequencies (Fig. 5b) corresponding to the boxed part in Figure 5a.

For $n = 3$ the normalized spectrum has its horizontal interval. With n increasing, ξ_n/n changes on this interval. Figure 5 demonstrates minor changes for $n = 30$ and a totally different behaviour for n equal to 150 and 301. So, for simulated large n, the low-frequency spectrum essentially deviates from ξ_3, as well as from ξ_{4k} for large k.

According to Figure 4 and 5, the long-time evolution of the sand-pile exhibits a great complexity. In contrast to the spatial features, the several patterns here discussed do not exhaust the spectrum behaviour. For the experiments made here, the sand-piles with deterministic and stochastic relaxation have different spectra.

5 Conclusion

To sum up, we have developed a family of sand-piles. The control parameter n is the number of grains that any unstable cell passes to its neighbours. For $n = 4k$, the propagation of grains through the lattice is fully deterministic, while the models with $n \neq 4k$ involve some random effect. In terms of the sand distribution, the random effect disappears when n is sufficiently large. However, a trace of the deterministic relaxation remains visible in the

spectrum of average height. A certain peak appears in the low-frequency spectrum. With their peculiar evolutionary properties, the sand-piles corresponding to deterministic relaxation may admit some kind of prediction. This hypothesis agrees with the effective precursors found for the BTW sand-pile in [27].

References

1. P. Bak, C. Tang, K. Wiesenfeld, Phys. Rev. Lett. **59**, 381 (1987)
2. P. Bak, C. Tang, K. Wiesenfeld, Phys. Rev. A **38**, 364 (1988)
3. D. Dhar, Phys. Rev. Lett. **64**, 1613 (1990)
4. D. Dhar, Physica A **263**, 4 (1999)
5. P. Grassberger, S.S. Manna, J. Phys. France **51**, 1077 (1990)
6. O. Biham, E. Milshtein, O. Malcai, Phys. Rev. E **63**, 061309 (2001)
7. D.V. Ktitarev, S. Lübeck, P. Grassberger, V.B. Priezzhev, Phys. Rev. E **61**, 81 (2000)
8. E.N. Miranda, H.J. Herrman, Phys. A **175**, 339 (1991)
9. P. Bak, C. Tang, J. Geophysical Res. **94**, 15635 (1987)
10. A. Bershadskii, K.R. Sreenivasan, Eur. Phys. J. B **35**, 513 (2003)
11. S.S. Manna, J. Stat. Phys. **59**, 509 (1990)
12. Y.C. Zhang, Phys. Rev. Lett. **63**, 470 (1989)
13. A. Ben-Hur, O. Biham, Phys. Rev. E **53**, R1317 (1996)
14. L. Pietronero, A. Vespignani, S. Zapperi, Phys. Rev. Lett. **72**, 1690 (1994)
15. A. Chessa, H.E. Stanley, A. Vespignani, S. Zapperi, Phys. Rev. E **59**, R12 (1999)
16. E.V. Ivashkevich, A.M. Povolotsky, A. Vespignani, S. Zapperi, Phys. Rev. E **60**, 1239 (1999)
17. C. Tebaldi, M. DeMenech, A.L. Stella, Phys. Rev. Lett. **83**, 3952 (1999)
18. S. Lübeck, Phys. Rev. E **61**, 204 (2000)
19. M. De Menech, A.L. Stella, Phys. Rev. E, **62**, R4528 (2000)
20. S. Lübeck, K.D. Usadel, Phys. Rev. E **55**, 4095 (1997)
21. S. Lübeck, Phys. Rev. E **62**, 6149 (2000)
22. A.B. Shapoval, M.G. Shnirman, Int. J. Mod. Phys. C **16** (2005)
23. P. de los Rios, Y. Zhang, Phys. Rev. **82**, 472 (1999)
24. R. Karmakar, S.S. Manna, A.L. Stella, Phys. Rev. Lett. **94**, 088002 (2005)
25. V.B. Priezzhev, J. Stat. Phys. **74**, 955 (1994)
26. M. DeMenech, A.L. Stella, C. Tebaldi, Phys. Rev. E **58**, R2677 (1998)
27. A.B. Shapoval, M.G. Shnirman, Int. J. Mod. Phys. C **15**, 279 (2004)